P. Hansbo and M. Juntunen. 2009. Weakly imposed Dirichlet boundary conditions for the Brinkman model of porous media flow. Applied Numerical Mathematics, volume 59, number 6, pages 1274-1289. doi:10.1016/j.apnum.2008.07.003.

Available online at www.sciencedirect.com

ScienceDirect

Applied Numerical Mathematics 59 (2009) 1274–1289

APPLIED NUMERICAL MATHEMATICS

www.elsevier.com/locate/apnum

Weakly imposed Dirichlet boundary conditions for the Brinkman model of porous media flow

P. Hansbo [a,*], M. Juntunen [b]

[a] *Department of Mathematical Sciences, Chalmers University of Technology and Göteborg University, SE-41296 Göteborg, Sweden*

[b] *Department of Engineering Physics and Mathematics, Institute of Mathematics, Helsinki University of Technology, P.O. Box 1100, 02015 TKK, Finland*

Available online 5 August 2008

Abstract

We use low order approximations, piecewise linear, continuous velocities and piecewise constant pressures to compute solutions to Brinkman's equation of porous media flow, applying an edge stabilization term to avoid locking. In order to handle the limiting case of Darcy flow, when only the velocity component normal to the boundary can be prescribed, we impose the boundary conditions weakly using Nitsche's method [J. Nitsche, Über ein Variationsprinzip zur Lösung von Dirichlet-Problemen bei Verwendung von Teilräumen, die keinen Randbedingungen unterworfen sind, Abhandlungen aus dem Mathematischen Seminar der Universität Hamburg 36 (1971) 9–15]. We show that this leads to a stable method for all choices of material parameters. Finally we present some numerical examples verifying the theoretical predictions and showing the effect of the weak imposition of boundary conditions.

Keywords: Brinkman model; Stokes–Darcy model; Stabilized methods; Finite element; Interior penalty method; Nitsche's method

1. Introduction

The Brinkman equations model creeping flow in porous media and can be seen as a mixture of Darcy's equations and Stokes' equations. The behavior of solutions to the Brinkman equations will be controlled by the ratio of permeability (in Darcy) to viscosity (Stokes), and it is desirable from a numerical point of view to develop methods that can handle the whole range of possible ratios, from the pure inviscid Darcy problem to the Stokes problem with full (infinite) permeability. In doing so, we are led to formulate the Darcy equations in mixed form using velocities and pressure as variables, as is done in the Stokes case. One problem that then arises is the fact that a good method for the Stokes problem may perform badly, or not even work, in the case of a mixed form of the Darcy problem, see Mardal, Tai, and Winther [9]. In [6], this problem was overcome by using a stabilized method that was shown to be convergent for both Darcy and Stokes; the same method will be used in the present study. Another inconvenient fact, from the point of view of numerical implementation, is that the Darcy equations do not admit the same boundary conditions as the Stokes equations: in the Darcy case only the velocity normal to the boundary can be prescribed, whereas no-slip boundary conditions are usually employed for Stokes. In this paper we suggest a remedy to this last inconvenience:

* Corresponding author.
E-mail addresses: peter.hansbo@me.chalmers.se (P. Hansbo), mika.juntunen@tkk.fi (M. Juntunen).

0168-9274/$30.00 © 2008 IMACS. Published by Elsevier B.V. All rights reserved.
doi:10.1016/j.apnum.2008.07.003

the use of weakly prescribed Dirichlet boundary conditions for the velocities using Nitsche's method [10]. The same approach was also used for Oseen's problem by Burman, Fernández, and Hansbo [5], but with a different focus.

Weakly imposed Dirichlet boundary conditions, first proposed for flow problems by Freund and Stenberg [7], have been shown to be advantageous for convection–diffusion problems with outflow layers, already in [7] and later in the work of Burman [3], in that it will lead to discontinuous jumps in the solution at the boundary rather than forcing a continuous numerical solution to mimic discontinuities. It has also been promoted by Bazilevs and Hughes [1] as an alternative to wall function models in turbulent channel flow, allowing for limited slip at the boundary. In these cases, the balance between a first order term (convection) and a second order term (diffusion/viscosity) is the factor that favors weak boundary conditions; in our case it is the balance between a zero order term (in Darcy) and a second order term (in Stokes). The idea is thus more general and its full potential awaits exploitation.

We will consider the following Brinkman model of porous flow

$$\begin{aligned} &\sigma \boldsymbol{u} - \nabla \cdot (\mu \nabla \boldsymbol{u}) + \nabla p = \boldsymbol{f} \quad \text{in } \Omega, \\ &\nabla \cdot \boldsymbol{u} = 0 \quad \text{in } \Omega, \end{aligned} \tag{1}$$

where Ω is an open, bounded subset of $\mathbb{R}^d$, $\boldsymbol{u}$ denotes the average fluid velocity in the porous medium, σ the viscosity divided by the permeability, μ the effective viscosity, p the pressure, and $\boldsymbol{f}$ is a given forcing term. We assume that Ω has polygonal boundary $\partial\Omega$ and that the boundary is divided into two non-overlapping sets $\partial\Omega = \Gamma_D \cup \Gamma_N$. The respective boundary conditions are

$$\begin{aligned} &\boldsymbol{u} = \boldsymbol{u}_0 \quad \text{on } \Gamma_D, \\ &\mu \partial_n \boldsymbol{u} - p\boldsymbol{n} = \boldsymbol{g} \quad \text{on } \Gamma_N, \end{aligned} \tag{2}$$

where $\boldsymbol{g} = g_n \boldsymbol{n} + \mu \boldsymbol{g}_t$, with g_n a scalar and $\boldsymbol{g}_t$ a vector in the plane perpendicular to $\boldsymbol{n}$. In other words we prescribe only the normal component of the Neumann condition in Darcy limit $\mu = 0$. Furthermore we assume that the measure of Γ_D is not zero i.e. we always have some Dirichlet boundary.

The side condition $\nabla \cdot \boldsymbol{u} = 0$ requires that some care is taken in the choice of approximating spaces in order to avoid over-constraining the problem. Here we shall use a stabilized scheme proposed for Stokes by Hughes and Franca [8], and for Darcy by Burman and Hansbo [6] (cf. also Burman [4] for a discussion of related methods). In this paper we apply this mixed stabilized method to the Brinkman equations with weakly imposed boundary conditions and prove optimal a priori estimates in the energy norm. We also give an *a posteriori* error estimate and adaptive algorithm for energy norm control of the computational error. Finally, we give some numerical examples showing the performance of the method and the adaptive algorithm.

2. Finite element formulation

In order to formulate our finite element method we first introduce the weak formulation of problem (1). We introduce the Hilbert spaces

$$W_{\boldsymbol{u}_0} = \left\{ \boldsymbol{v} \in \left[H^1(\Omega) \right]^d \text{ s.t. } \boldsymbol{v}_{|\Gamma_D} = \boldsymbol{u}_0 \right\},$$

and

$$L_0^2 = \left\{ q \in L^2(\Omega) \text{ s.t. } \int_\Omega q \,\mathrm{d}x = 0 \right\}.$$

We denote the product space $W_{\boldsymbol{u}_0} \times L_0^2$ by $\mathcal{W}_{\boldsymbol{u}_0}$ and define the following norm on $\mathcal{W}_{\boldsymbol{u}_0}$,

$$\left\| (\boldsymbol{u}, p) \right\|_{\mathcal{W}}^2 = \sigma \|\boldsymbol{u}\|_{0,\Omega}^2 + \mu \|\boldsymbol{u}\|_{1,\Omega}^2 + \|\nabla \cdot \boldsymbol{u}\|_{0,\Omega}^2 + \|p\|_{0,\Omega}^2.$$

Consider the bilinear form

$$B\big[(\boldsymbol{u}, p), (\boldsymbol{v}, q)\big] = (\mu \nabla \boldsymbol{u}, \nabla \boldsymbol{v})_{0,\Omega} + (\sigma \boldsymbol{u}, \boldsymbol{v})_{0,\Omega} - (p, \nabla \cdot \boldsymbol{v})_{0,\Omega} - (q, \nabla \cdot \boldsymbol{u})_{0,\Omega}. \tag{3}$$

The weak formulation of (1) now takes the form, find $(\boldsymbol{u}, p) \in \mathcal{W}_{\boldsymbol{u}_0}$ such that

$$B\big[(\boldsymbol{u}, p), (\boldsymbol{v}, q)\big] = (\boldsymbol{f}, \boldsymbol{v})_{0,\Omega} + (\boldsymbol{g}, \boldsymbol{v})_{0,\Gamma_N} \quad \forall (\boldsymbol{v}, q) \in \mathcal{W}_0. \tag{4}$$

Let $\mathcal{T}^h$ be a conforming, shape regular triangulation of Ω. With K we denote an element of the triangulation and with E an edge/face of the triangulation. By h_K and h_E we denote the size of an element or edge/face, respectively, and by h we denote the size of the largest element in $\mathcal{T}^h$. We introduce the two classical finite element spaces of piecewise linears and piecewise constants

$$V^h = \{v \text{ s.t. } v_{|K} \in P_1(K),\ v \in C^0(\Omega)\},$$
$$Q^h = \left\{q \text{ s.t. } q_{|K} \in P_0(K),\ \int_\Omega q\,\mathrm{d}x = 0\right\}.$$

The velocity field will be sought in $W^h = [V^h]^d$ and the pressure field in Q^h. In analogy with the notation above we use the notation $\mathcal{W}^h := W^h \times Q^h$. We introduce the following bilinear and linear forms on which we will base our finite element method:

$$\begin{aligned} B^h[(\boldsymbol{u},p),(\boldsymbol{v},q)] = {} & (\mu\nabla\boldsymbol{u},\nabla\boldsymbol{v})_{0,\Omega} + (\sigma\boldsymbol{u},\boldsymbol{v})_{0,\Omega} - (p,\nabla\cdot\boldsymbol{v})_{0,\Omega} - (q,\nabla\cdot\boldsymbol{u})_{0,\Omega} - J^h(p,q) \\ & - (\mu\partial_n\boldsymbol{u},\boldsymbol{v})_{0,\Gamma_D} - (\mu\boldsymbol{u},\partial_n\boldsymbol{v})_{0,\Gamma_D} + (\mu\gamma_\mu h^{-1}\boldsymbol{u},\boldsymbol{v})_{0,\Gamma_D} \\ & + (p,\boldsymbol{v}\cdot\boldsymbol{n})_{0,\Gamma_D} + (\boldsymbol{u}\cdot\boldsymbol{n},q)_{0,\Gamma_D} + (\gamma_\sigma h^{-1}\boldsymbol{u}\cdot\boldsymbol{n},\boldsymbol{v}\cdot\boldsymbol{n})_{0,\Gamma_D} \end{aligned} \tag{5}$$

and

$$\begin{aligned} L^h[(\boldsymbol{v},q)] := {} & (\boldsymbol{f},\boldsymbol{v})_{0,\Omega} + (\boldsymbol{g},\boldsymbol{v})_{0,\Gamma_N} - (\boldsymbol{u}_0,\partial_n v)_{0,\Gamma_D} + (\boldsymbol{u}_0,\mu\gamma_\mu h^{-1} v)_{0,\Gamma_D} \\ & + (\boldsymbol{u}_0\cdot\boldsymbol{n},q)_{0,\Gamma_D} + (\boldsymbol{u}_0\cdot\boldsymbol{n},\gamma_\sigma h^{-1}\boldsymbol{v}\cdot\boldsymbol{n})_{0,\Gamma_D}, \end{aligned} \tag{6}$$

where

$$J^h(p,q) = \delta \sum_{(E\in\mathcal{T}^h)\setminus\partial\Omega} h_E([p],[q])_{0,E}, \tag{7}$$

with $[\cdot]$ denoting the jump over the element edge (taken on the interior edges only). Above, and in what follows, in the inner product $h = h(x)$ i.e. h correspond to the element under integration, not to the global maximum. We propose the following finite element formulation: find $(\boldsymbol{u}^h, p^h) \in \mathcal{W}^h$ such that

$$B^h[(\boldsymbol{u}^h,p^h),(\boldsymbol{v}^h,q^h)] = L^h[(\boldsymbol{v}^h,q)] \quad \forall(\boldsymbol{v}^h,q^h)\in\mathcal{W}^h. \tag{8}$$

This finite element formulation is simply the standard Galerkin formulation with Nitsche boundary conditions and the penalizing term $J^h(p,q)$ added. In the following we will assume that the pressure is in $H^1(\Omega)$: then the penalizing term is consistent and we have the following

Lemma 2.1. *If* $(\boldsymbol{u}, p)$ *is a weak solution to* (1) *with* $(\boldsymbol{u}, p) \in W \times H^1(\Omega) \cap L^2_0$ *then*

$$B^h[(\boldsymbol{u}-\boldsymbol{u}^h,p-p^h),(\boldsymbol{v}^h,q^h)] = 0 \quad \forall(\boldsymbol{v}^h,q^h)\in\mathcal{W}^h. \tag{9}$$

Proof. Immediate by noting that if $p \in H^1(\Omega)$ then the trace of p is well defined and hence $J^h(p, q^h) = 0$ for all $q^h \in Q^h$. □

3. Stability

Since it is a well known fact that the above choice of finite element spaces results in an ill posed discrete problem if used in a standard Galerkin method, the crucial point is to show that our stabilization operator $J^h(p,q)$ introduces sufficient coupling between the degrees of freedom in the pressure field such that an *inf–sup* condition is satisfied. This was done for Darcy in [6], using the standard way of handling Dirichlet boundary conditions. Here, we extend the analysis of [6] to the Brinkman model with weakly imposed Dirichlet boundary conditions.

In the analysis, we will use the following norms:

$$\|(\boldsymbol{u},p)\|_h^2 := \|(\boldsymbol{u},p)\|_{\mathcal{W}}^2 + J^h(p,p) + \mu\|\boldsymbol{u}\|_{1/2,h,\Gamma_D}^2 + \|\boldsymbol{u}\cdot\boldsymbol{n}\|_{1/2,h,\Gamma_D}^2, \tag{10}$$

$$|||(\boldsymbol{u},p)|||_h^2 := \|(\boldsymbol{u},p)\|_h^2 + \mu\|\boldsymbol{u}\|_{-1/2,h,\Gamma_D}^2, \tag{11}$$

where

$$\|v\|^2_{1/2,h,\Gamma_D} := \left(h^{-1} v, v\right)_{0,\Gamma_D} \quad \text{and} \quad \|v\|^2_{-1/2,h,\Gamma_D} := (h\, v, v)_{0,\Gamma_D}.$$

Note that the norms contain the L^2-norm of $\nabla \cdot \boldsymbol{u}$; this term is superfluous for Stokes since we already control the H^1-norm of the velocities, but of vital importance for Darcy. In fact, the control of the divergence is what allows us to prove optimal error estimates in the energy norm for sufficiently regular solutions. In what follows we will use the following well known estimates:

$$(\partial_n \boldsymbol{v}, \boldsymbol{w})_{0,\partial\Omega} \leqslant \|\partial_n \boldsymbol{v}\|_{-1/2,h,\partial\Omega} \|\boldsymbol{w}\|_{1/2,h,\partial\Omega} \quad \forall \boldsymbol{v}, \boldsymbol{w} \in V^h, \tag{12}$$

$$\|\partial_n \boldsymbol{v}\|^2_{-1/2,h,\partial\Omega} \leqslant C_I \|\nabla \boldsymbol{v}\|^2_{0,\Omega} \quad \forall \boldsymbol{v} \in V^h, \tag{13}$$

$$\|\nabla \cdot \boldsymbol{v}\|^2_{-1/2,h,\partial\Omega} \leqslant C_{II} \|\nabla \cdot \boldsymbol{v}\|^2_{0,\Omega} \quad \forall \boldsymbol{v} \in V^h. \tag{14}$$

Note that due to estimate (13) the norms $\|\cdot\|_h$ and $|||\cdot|||_h$ are equivalent on the finite element subspace.

In the following, we will let C denote a generic positive constant whose value may change from instance to instance.

The main result of this section is the following theorem, assuring the well-posedness of our discretization.

Theorem 3.1. *Assume $\gamma_\mu > C_I$ and $\gamma_\sigma > 0$. Then the finite element formulation* (8) *satisfies the following* inf–sup *condition*

$$\alpha \left\| \left(\boldsymbol{u}^h, p^h\right) \right\|_h \leqslant \sup_{(\boldsymbol{v}^h, q^h) \in \mathcal{W}^h} \frac{B^h[(\boldsymbol{u}^h, p^h), (\boldsymbol{v}^h, q^h)]}{\|(\boldsymbol{v}^h, q^h)\|_h}, \quad \forall \left(\boldsymbol{u}^h, p^h\right) \in \mathcal{W}^h.$$

Proof. The idea of the proof is to acquire control of the different terms of the energy norm with different choices of test functions and finally combine the choices using the linearity of the bilinear form.

Step 1. Taking first $(\boldsymbol{v}^h, q^h) = (\boldsymbol{u}^h, -p^h)$ we obtain

$$\begin{aligned} B^h\left[\left(\boldsymbol{u}^h, p^h\right), \left(\boldsymbol{u}^h, -p^h\right)\right] &= \mu \left\|\nabla \boldsymbol{u}^h\right\|^2_{0,\Omega} + \sigma \left\|\boldsymbol{u}^h\right\|^2_{0,\Omega} + J^h\left(p^h, p^h\right) - 2\left(\mu \partial_n \boldsymbol{u}^h, \boldsymbol{u}^h\right)_{0,\Gamma_D} \\ &\quad + \gamma_\mu \mu \left\|\boldsymbol{u}^h\right\|^2_{1/2,h,\Gamma_D} + \gamma_\sigma \left\|\boldsymbol{u}^h \cdot \boldsymbol{n}\right\|^2_{1/2,h,\Gamma_D}. \end{aligned}$$

Using Young's inequality and estimates (12) and (13) we get

$$\begin{aligned} B^h\left[\left(\boldsymbol{u}^h, p^h\right), \left(\boldsymbol{u}^h, -p^h\right)\right] &\geqslant \left(1 - \frac{C_I}{\epsilon}\right) \mu \left\|\nabla \boldsymbol{u}^h\right\|^2_{0,\Omega} + \sigma \left\|\boldsymbol{u}^h\right\|^2_{0,\Omega} + J^h\left(p^h, p^h\right) \\ &\quad + (\gamma_\mu - \epsilon) \mu \left\|\boldsymbol{u}^h\right\|^2_{1/2,h,\Gamma_D} + \gamma_\sigma \left\|\boldsymbol{u}^h \cdot \boldsymbol{n}\right\|^2_{1/2,h,\Gamma_D}, \end{aligned}$$

where $\epsilon > 0$ is a parameter from Young's inequality. Our assumption is that $\gamma_\mu > C_I$. Therefore we can choose $C_I < \epsilon < \gamma_\mu$ and we have

$$\begin{aligned} B^h\left[\left(\boldsymbol{u}^h, p^h\right), \left(\boldsymbol{u}^h, -p^h\right)\right] &\geqslant C_1 \mu \left\|\nabla \boldsymbol{u}^h\right\|^2_{0,\Omega} + \sigma \left\|\boldsymbol{u}^h\right\|^2_{0,\Omega} + J^h\left(p^h, p^h\right) \\ &\quad + C_2 \mu \left\|\boldsymbol{u}^h\right\|^2_{1/2,h,\Gamma_D} + \gamma_\sigma \left\|\boldsymbol{u}^h \cdot \boldsymbol{n}\right\|^2_{1/2,h,\Gamma_D}. \end{aligned} \tag{15}$$

Step 2. We are still missing the control of the pressure and the divergence of the velocity. To gain control over the pressure we note that as a consequence of the surjectivity of the divergence operator there exists a function $\boldsymbol{v}_p \in [H^1_0(\Omega)]^d$ such that $\nabla \cdot \boldsymbol{v}_p = p^h$ and

$$\|\boldsymbol{v}_p\|_{1,\Omega} \leqslant C \left\|p^h\right\|_{0,\Omega}. \tag{16}$$

Let $\pi^h \boldsymbol{v}_p$ denote the Scott–Zhang interpolant (cf. [2]) of $\boldsymbol{v}_p$ onto $[V^h_0]^d$, where

$$V^h_0 := \left\{v \text{ s.t. } v_{|K} \in P_1(K),\ v \in C^0(\Omega),\ v = 0 \text{ on } \partial\Omega\right\}.$$

By the stability of the interpolant we have

$$\left\|\pi^h \boldsymbol{v}_p\right\|_{1,\Omega} \leqslant \tilde{c} \left\|p^h\right\|_{0,\Omega}. \tag{17}$$

We now choose the test function to be $(\boldsymbol{v}^h, q^h) = (-\pi^h \boldsymbol{v}_p, 0)$. Adding

$$0 = \|p^h\|_{0,\Omega}^2 - (p^h, \nabla\cdot \boldsymbol{v}_p)_{0,\Omega}$$

and recalling that $\pi^h \boldsymbol{v}_p$ vanishes on the boundary we obtain

$$\begin{aligned} B^h\big[(\boldsymbol{u}^h, p^h), (-\pi^h \boldsymbol{v}_p, 0)\big] = {} & -\mu(\nabla \boldsymbol{u}^h, \nabla \pi^h \boldsymbol{v}_p)_{0,\Omega} - \sigma(\boldsymbol{u}^h, \pi^h \boldsymbol{v}_p)_{0,\Omega} + \|p^h\|_{0,\Omega}^2 \\ & + \big(p^h, \nabla\cdot(\pi^h \boldsymbol{v}_p - \boldsymbol{v}_p)\big)_{0,\Omega} + \mu(\boldsymbol{u}^h, \partial_n \pi^h \boldsymbol{v}_p)_{0,\Gamma_D}. \end{aligned}$$

Integrating the fourth term by parts on each element K we get

$$\begin{aligned} B^h\big[(\boldsymbol{u}^h, p^h), (\pi^h \boldsymbol{v}_p, 0)\big] = {} & -\mu(\nabla \boldsymbol{u}^h, \nabla \pi^h \boldsymbol{v}_p)_{0,\Omega} - \sigma(\boldsymbol{u}^h, \pi^h \boldsymbol{v}_p)_{0,\Omega} + \|p^h\|_{0,\Omega}^2 \\ & + \sum_{K\in\mathcal{T}^h} \frac{1}{2}\big([p^h], (\pi^h \boldsymbol{v}_p - \boldsymbol{v}_p)\cdot \boldsymbol{n}\big)_{0,\partial K} + \mu(\boldsymbol{u}^h, \partial_n \pi^h \boldsymbol{v}_p)_{0,\Gamma_D}. \end{aligned}$$

Splitting the inner products using Schwarz inequality, followed by Young's inequality, we have

$$\begin{aligned} B^h\big[(\boldsymbol{u}^h, p^h), (\pi^h \boldsymbol{v}_p, 0)\big] \geqslant {} & -\frac{1}{2\epsilon}\mu\|\nabla \boldsymbol{u}^h\|_{0,\Omega}^2 - \frac{\epsilon}{2}\mu\|\nabla\pi^h \boldsymbol{v}_p\|_{0,\Omega}^2 - \frac{1}{2\epsilon}\sigma\|\boldsymbol{u}^h\|_{0,\Omega}^2 - \frac{\epsilon}{2}\sigma\|\pi^h \boldsymbol{v}_p\|_{0,\Omega}^2 \\ & + \|p^h\|_{0,\Omega}^2 - \frac{1}{2\epsilon}\mu\|\boldsymbol{u}^h\|_{1/2,h,\Gamma_D}^2 - \frac{\epsilon}{2}\mu\|\partial_n \pi^h \boldsymbol{v}_p\|_{-1/2,h,\Gamma_D}^2 \\ & - \frac{1}{2\delta\epsilon} J^h(p^h, p^h) - \frac{\epsilon}{2}\sum_{(E\in\mathcal{T}^h)\setminus\partial\Omega} h_E \big\|(\pi^h \boldsymbol{v}_p - \boldsymbol{v}_p)\cdot \boldsymbol{n}\big\|_{0,E}^2. \end{aligned}$$

Using estimate (13) and the stability of the interpolate (17) we get

$$\begin{aligned} B^h\big[(\boldsymbol{u}^h, p^h), (\pi^h \boldsymbol{v}_p, 0)\big] \geqslant {} & -\frac{1}{2\epsilon}\mu\|\nabla \boldsymbol{u}^h\|_{0,\Omega}^2 - \frac{1}{2\epsilon}\sigma\|\boldsymbol{u}^h\|_{0,\Omega}^2 + \left(1 - \frac{\epsilon}{2}(\mu\tilde{c} + \sigma\tilde{c} + \mu\tilde{c}C_I)\right)\|p^h\|_{0,\Omega}^2 \\ & - \frac{1}{2\epsilon}\mu\|\boldsymbol{u}^h\|_{1/2,h,\Gamma_D}^2 - \frac{1}{2\delta\epsilon} J^h(p^h, p^h) - \frac{\epsilon}{2}\sum_{(E\in\mathcal{T}^h)\setminus\partial\Omega} h_E\big\|(\pi^h \boldsymbol{v}_p - \boldsymbol{v}_p)\cdot \boldsymbol{n}\big\|_{0,E}^2. \end{aligned}$$

To conclude we need the following trace inequality, cf. [11],

$$\|\boldsymbol{w}\cdot \boldsymbol{n}\|_{0,\partial K}^2 \leqslant C\big(h^{-1}\|\boldsymbol{w}\|_{0,K}^2 + h\|\boldsymbol{w}\|_{1,K}^2\big) \quad \forall \boldsymbol{w} \in \big[H^1(K)\big]^d, \tag{18}$$

from which we deduce, using (16),

$$\sum_{(E\in\mathcal{T}^h)\setminus\partial\Omega} h_E\big\|(\pi^h \boldsymbol{v}_p - \boldsymbol{v}_p)\cdot \boldsymbol{n}\big\|_{0,E}^2 \leqslant C\sum_{K\in\mathcal{T}^h}\|\boldsymbol{v}_p\|_{1,\Omega}^2 \leqslant C\|p^h\|_{0,\Omega}^2.$$

Using the inequality above we obtain

$$\begin{aligned} B^h\big[(\boldsymbol{u}^h, p^h), (\pi^h \boldsymbol{v}_p, 0)\big] \geqslant {} & -\frac{1}{2\epsilon}\mu\|\nabla \boldsymbol{u}^h\|_{0,\Omega}^2 - \frac{1}{2\epsilon}\sigma\|\boldsymbol{u}^h\|_{0,\Omega}^2 + \left(1 - \frac{\epsilon}{2}(\mu\tilde{c} + \sigma\tilde{c} + \mu\tilde{c}C_I + C)\right)\|p^h\|_{0,\Omega}^2 \\ & - \frac{1}{2\epsilon}\mu\|\boldsymbol{u}^h\|_{1/2,h,\Gamma_D}^2 - \frac{1}{2\delta\epsilon} J^h(p^h, p^h). \end{aligned}$$

Setting $0 < \epsilon < 2/(\mu\tilde{c} + \sigma\tilde{c} + \mu\tilde{c}C_I + C)$ we finally have

$$\begin{aligned} B^h\big[(\boldsymbol{u}^h, p^h), (\pi^h \boldsymbol{v}_p, 0)\big] \geqslant {} & -C_3\mu\|\nabla \boldsymbol{u}^h\|_{0,\Omega}^2 - C_3\sigma\|\boldsymbol{u}^h\|_{0,\Omega}^2 + C_4\|p^h\|_{0,\Omega}^2 \\ & - C_3\mu\|\boldsymbol{u}^h\|_{1/2,h,\Gamma_D}^2 - \frac{C_3}{\delta} J^h(p^h, p^h). \end{aligned} \tag{19}$$

Step 3. The divergence of the velocity is already contained in the H^1–norm of the velocity if $\mu > 0$ but we want to have the control of the divergence even if $\mu = 0$.

The control of $\|\nabla\cdot \boldsymbol{u}^h\|_{0,\Omega}^2$ is obtained choosing $(\boldsymbol{v}^h, q^h) = (0, -\nabla\cdot \boldsymbol{u}^h)$, which leads to

$$B^h\big[(\boldsymbol{u}^h, p^h), (0, -\nabla\cdot\boldsymbol{u}^h)\big] = \|\nabla\cdot\boldsymbol{u}^h\|_{0,\Omega}^2 + J^h(p^h, \nabla\cdot\boldsymbol{u}^h) - (\nabla\cdot\boldsymbol{u}^h, \boldsymbol{u}^h\cdot\boldsymbol{n})_{0,\Gamma_D}$$
$$\geqslant \|\nabla\cdot\boldsymbol{u}^h\|_{0,\Omega}^2 - \sum_{(E\in\mathcal{T}^h)\setminus\partial\Omega}\frac{\xi}{2}\delta\|\nabla\cdot\boldsymbol{u}^h\|_{-1/2,h,E}^2 - \frac{1}{2\xi}J^h(p^h, p^h)$$
$$-\frac{\xi}{2}\|\nabla\cdot\boldsymbol{u}^h\|_{-1/2,h,\Gamma_D}^2 - \frac{1}{2\xi}\|\boldsymbol{u}^h\cdot\boldsymbol{n}\|_{1/2,h,\Gamma_D}^2.$$

Using estimate (14) we get

$$B^h\big[(\boldsymbol{u}^h, p^h), (0, -\nabla\cdot\boldsymbol{u}^h)\big] \geqslant \left(1 - \frac{\xi}{2}C_{II}(1+\delta)\right)\|\nabla\cdot\boldsymbol{u}^h\|_{0,\Omega}^2 - \frac{1}{2\xi}J^h(p^h, p^h) - \frac{1}{2\xi}\|\boldsymbol{u}^h\cdot\boldsymbol{n}\|_{1/2,h,\Gamma_D}^2. \tag{20}$$

Step 4. Now we have control over all the terms in the energy norm separately. Finally we take $(\boldsymbol{v}^h, q^h) = (\beta\boldsymbol{u}^h - \pi^h\boldsymbol{v}_p, \beta p^h - \nabla\cdot\boldsymbol{u}^h)$. Combining the results (15), (19) and (20) we get

$$B^h\big[(\boldsymbol{u}^h, p^h), (\boldsymbol{v}^h, q^h)\big] \geqslant (\beta C_1 - C_3)\mu\|\nabla\boldsymbol{u}^h\|_{0,\Omega}^2 + (\beta - C_3)\sigma\|\boldsymbol{u}^h\|_{0,\Omega}^2 + C_4\|p^h\|_{0,\Omega}^2$$
$$+ \left(1 - \frac{\xi}{2}C_{II}(1+\delta)\right)\|\nabla\cdot\boldsymbol{u}^h\|_{0,\Omega}^2 + \left(\beta - \frac{1}{2\xi} - \frac{C_3}{\delta}\right)J^h(p^h, p^h)$$
$$+ (\beta C_2 - C_3)\mu\|\boldsymbol{u}^h\|_{1/2,h,\Gamma_D}^2 + \left(\beta\gamma_0 - \frac{1}{2\xi}\right)\|\boldsymbol{u}^h\cdot\boldsymbol{n}\|_{1/2,h,\Gamma_D}^2.$$

The fourth term on the right-hand side is positive if the parameter from Young's inequality is $\xi < 2/(C_{II}(1+\delta))$. With this the rest of the terms are positive if $\beta > C_3/C_1$, $\beta > C_3$, $\beta > C_{II}(1+\delta) + C_3/\delta$, $\beta > C_3/C_2$, and $\beta > C_{II}(1+\delta)/\gamma_0$. Then we have that

$$B^h\big[(\boldsymbol{u}^h, p^h), (\boldsymbol{v}^h, q^h)\big] \geqslant \big|\!\big|\!\big|(\boldsymbol{u}^h, p^h)\big|\!\big|\!\big|_h^2$$

and the claim follows since there exists $C > 0$ such that $|||(\boldsymbol{u}^h, p^h)|||_h \geqslant C|||(\boldsymbol{v}^h, q^h)|||_h$. □

Note that the Nitsche stability parameter γ_σ forcing the Darcy problems boundary conditions has no lower bound. This holds even on Darcy limit $\mu = 0$.

In the rest of the paper we assume that the stability requirement is satisfied, i.e. we make the following assumption.

Assumption 3.2. The real parameter γ_μ satisfies $\gamma_\mu > C_I$.

4. Error analysis

4.1. A priori estimates

First of all, we note that applying the trace inequality (18) we easily derive the following approximation property for couples of functions $(\boldsymbol{u}, p) \in [H^2(\Omega)]^d \times H^1(\Omega)$,

$$\big|\!\big|\!\big|(\boldsymbol{u} - \pi^h\boldsymbol{u}, p - \pi^h p)\big|\!\big|\!\big|_h \leqslant Ch\big(\|\boldsymbol{u}\|_{2,\Omega} + \|p\|_{1,\Omega}\big), \tag{21}$$

where $(\pi^h\boldsymbol{u}, \pi^h p) \in \mathcal{W}^h$ denotes the interpolates. Without proof we also state the continuity of the bilinear form.

Lemma 4.1. *For all $(\boldsymbol{u}, p), (\boldsymbol{v}, q) \in \mathcal{W}$ it holds*

$$B^h\big[(\boldsymbol{u}, p), (\boldsymbol{v}, q)\big] \leqslant C\big|\!\big|\!\big|(\boldsymbol{u}, p)\big|\!\big|\!\big|_h\big|\!\big|\!\big|(\boldsymbol{v}, q)\big|\!\big|\!\big|_h. \tag{22}$$

The main result in this section is the following lemma.

Lemma 4.2. *Assume that the solution $(\boldsymbol{u}, p)$ to the problem* (1) *resides in $[H^2(\Omega)]^d \times H^1(\Omega) \cap L_0^2(\Omega)$; then the finite element solution* (8) *satisfies the error estimate*

$$\big\|(\boldsymbol{u} - \boldsymbol{u}^h, p - p^h)\big\|_h \leqslant Ch\big(\|\boldsymbol{u}\|_{2,\Omega} + \|p\|_{1,\Omega}\big).$$

Proof. In view of the approximation property (21) we only need to show the inequality for $|||(\boldsymbol{u}^h - \pi^h \boldsymbol{u}, p^h - \pi^h p)|||$. By the stability, see Theorem 3.1, there exist a pair $(\boldsymbol{v}^h, q^h) \in \mathcal{W}^h$ such that $\|(\boldsymbol{v}^h, q^h)\|_h = 1$ and

$$\|(\boldsymbol{u}^h - \pi^h \boldsymbol{u}, p^h - \pi^h p)\|_h \leqslant \alpha^{-1} B^h[(\boldsymbol{u}^h - \pi^h \boldsymbol{u}, p^h - \pi^h p), (\boldsymbol{v}^h, q^h)].$$

Using the Galerkin orthogonality, see Lemma 2.1, we obtain

$$\|(\boldsymbol{u}^h - \pi^h \boldsymbol{u}, p^h - \pi^h p)\|_h \leqslant \alpha^{-1} B^h[(\boldsymbol{u} - \pi^h \boldsymbol{u}, p - \pi^h p), (\boldsymbol{v}^h, q^h)].$$

Furthermore, using the continuity of the bilinear form, Eq. (22), and recalling that the energy norms are equivalent in the finite element subspace, we have

$$\|(\boldsymbol{u}^h - \pi^h \boldsymbol{u}, p^h - \pi^h p)\|_h \leqslant \alpha^{-1} C |||(\boldsymbol{u} - \pi^h \boldsymbol{u}, p - \pi^h p)|||_h.$$

Now the claim follows by the approximation property (21). □

4.2. *A posteriori estimate*

In this section we propose and prove the a posteriori estimate in the energy norm. In what follows we will need two meshes. The original mesh $\mathcal{T}^h$ and mesh $\mathcal{T}^{h/2}$ derived from the original mesh by splitting the elements. By pair $(\boldsymbol{u}^h, p^h)$ we denote the solution on the mesh $\mathcal{T}^h$ and by $(\boldsymbol{u}^{h/2}, p^{h/2})$ the solution on the mesh $\mathcal{T}^{h/2}$. The proof is based on the following saturation assumption.

Assumption 4.3 *(Saturation assumption).* There exists $0 < \beta < 1$ such that

$$\|(\boldsymbol{u} - \boldsymbol{u}^{h/2}, p - p^{h/2})\|_{h/2} \leqslant \beta \|(\boldsymbol{u} - \boldsymbol{u}^h, p - p^h)\|_h. \tag{23}$$

We note that this assumption is asymptotic in nature and cannot be expected to hold is there are unresolved features in the flow. However, this does not mean that unresolved features will not be detected (being a residual-based estimate it will still signal large errors where the residual is large), only that there will be a lack of sharpness of the estimate outside the asymptotic range.

The residual based elementwise estimator is defined as

$$\begin{aligned} E_K[(\boldsymbol{u}^h, p^h)]^2 := {} & \frac{h_K^2}{\mu + \sigma h_K^2} \|\nabla \cdot \mu \nabla \boldsymbol{u}^h - \sigma \boldsymbol{u}^h - \widehat{\nabla} p^h + \boldsymbol{f}\|_{0,K}^2 + \|\nabla \cdot \boldsymbol{u}^h\|_{0,K}^2 \\ & + \mu h_E \|[\partial_n \boldsymbol{u}^h]\|_{0,\partial K \setminus \partial\Omega}^2 + h_E \|[p^h]\|_{0,\partial K \setminus \partial\Omega}^2 \\ & + \mu h_E \|\boldsymbol{g}_t - \partial_n \boldsymbol{u}^h + (\partial_n \boldsymbol{u}^h \cdot \boldsymbol{n})\boldsymbol{n}\|_{0,\partial K \cap \Gamma_N}^2 + \mu h_E^{-1} \|\boldsymbol{u}_0 - \boldsymbol{u}^h\|_{0,\partial K \cap \Gamma_D}^2 \\ & + h_E \|g_n + p^h - \mu \partial_n \boldsymbol{u}^h \cdot \boldsymbol{n}\|_{0,\partial K \cap \Gamma_N}^2 + h_E^{-1} \|\boldsymbol{u}_0 \cdot \boldsymbol{n} - \boldsymbol{u}^h \cdot \boldsymbol{n}\|_{0,\partial K \cap \Gamma_D}^2, \end{aligned} \tag{24}$$

where the approximate gradient of pressure $\widehat{\nabla} p^h \in W^h$ is defined as the solution to

$$(-\widehat{\nabla} p^h, \boldsymbol{v})_{0,\Omega} = (p^h, \nabla \cdot \boldsymbol{v})_{0,\Omega} - (p^h, \boldsymbol{v} \cdot \boldsymbol{n})_{0,\partial\Omega} \quad \forall \boldsymbol{v} \in W^h. \tag{25}$$

We then have the following result.

Theorem 4.4. *Under the Assumptions* 3.2 *and* 4.3 *it holds*

$$\|(\boldsymbol{u} - \boldsymbol{u}^h, p - p^h)\|_h \leqslant C \Big(\sum_{K \in \mathcal{T}^h} E_K[(\boldsymbol{u}^h, p^h)]^2 \Big)^{1/2}. \tag{26}$$

Proof.

Step 1. By the triangle inequality and the saturation Assumption 4.3 we have

$$\|(\boldsymbol{u} - \boldsymbol{u}^h, p - p^h)\|_h \leqslant \frac{1}{1-\beta} \|(\boldsymbol{u}^{h/2} - \boldsymbol{u}^h, p^{h/2} - p^h)\|_{h/2}. \tag{27}$$

Hence it is sufficient to bound $\|(\boldsymbol{u}^{h/2}-\boldsymbol{u}^h, p^{h/2}-p^h)\|_{h/2}$. By the stability, Theorem 3.1, we know that there exists $(\boldsymbol{v}^{h/2}, q^{h/2}) \in \mathcal{W}^{h/2}$ such that

$$\alpha \big\| \big(\boldsymbol{u}^{h/2}-\boldsymbol{u}^h, p^{h/2}-p^h\big) \big\|_{h/2} \leqslant B^{h/2}\big[\big(\boldsymbol{u}^{h/2}-\boldsymbol{u}^h, p^{h/2}-p^h\big), \big(\boldsymbol{v}^{h/2}, q^{h/2}\big)\big] \tag{28}$$

and $\|(\boldsymbol{v}^{h/2}, q^{h/2})\|_{h/2} = 1$. Let $(\boldsymbol{v}^h, q^h) \in \mathcal{W}^h$ be an interpolate to $(\boldsymbol{v}^{h/2}, q^{h/2}) \in \mathcal{W}^{h/2}$. To simplify the notation we denote

$$\boldsymbol{w} := \boldsymbol{v}^{h/2} - \boldsymbol{v}^h \quad \text{and} \quad r := q^{h/2} - q^h.$$

By scaling arguments one obtains

$$\sum_{K \in \mathcal{T}^{h/2}} \big\{ \big(\sigma + \mu h_K^{-2}\big) \|\boldsymbol{w}\|_{0,K}^2 + \|\nabla \cdot \boldsymbol{w}\|_{0,K}^2 + \|r\|_{0,K}^2 + \mu h_K \|\partial_n \boldsymbol{w}\|_{0,\partial K}^2 \\ + h_K \|r\|_{0,\partial K}^2 + \mu h_K^{-1} \|\boldsymbol{w}\|_{\partial K}^2 + h_K^{-1} \|\boldsymbol{w} \cdot \boldsymbol{n}\|_{\partial K}^2 \big\} \leqslant C \big\| \big(\boldsymbol{v}^{h/2}, q^{h/2}\big) \big\|_{h/2}^2 \leqslant C. \tag{29}$$

Combining Eqs. (27) and (28), and using the interpolate to split the bilinear form into two parts, we get

$$\begin{aligned} C \big\| \big(\boldsymbol{u}-\boldsymbol{u}^h, p-p^h\big) \big\|_h &\leqslant B^{h/2}\big[\big(\boldsymbol{u}^{h/2}-\boldsymbol{u}^h, p^{h/2}-p^h\big), \big(\boldsymbol{v}^{h/2}, q^{h/2}\big)\big] \\ &= B^{h/2}\big[\big(\boldsymbol{u}^{h/2}-\boldsymbol{u}^h, p^{h/2}-p^h\big), (\boldsymbol{w}, r)\big] + B^{h/2}\big[\big(\boldsymbol{u}^{h/2}-\boldsymbol{u}^h, p^{h/2}-p^h\big), \big(\boldsymbol{v}^h, q^h\big)\big] \\ &= W_1 + W_2. \end{aligned} \tag{30}$$

Step 2. We bound the terms W_1 and W_2 separately, starting with W_1. Since $(\boldsymbol{u}^{h/2}, p^{h/2})$ is the solution to the problem, we have

$$\begin{aligned} W_1 &= L^{h/2}\big[(\boldsymbol{w}, r)\big] - B^{h/2}\big[\big(\boldsymbol{u}^h, p^h\big), (\boldsymbol{w}, r)\big] \\ &= (\boldsymbol{f}, \boldsymbol{w})_{0,\Omega} + (\boldsymbol{g}, \boldsymbol{w})_{0,\Gamma_N} + \big(\boldsymbol{u}_0, \gamma_\mu \mu 2h^{-1} \boldsymbol{w}\big)_{0,\Gamma_D} - (\boldsymbol{u}_0, \mu \partial_n \boldsymbol{w})_{0,\Gamma_D} + \big(\boldsymbol{u}_0 \cdot \boldsymbol{n}, \gamma_\sigma 2h^{-1} \boldsymbol{w} \cdot \boldsymbol{n}\big)_{0,\Gamma_D} \\ &\quad + (\boldsymbol{u}_0 \cdot \boldsymbol{n}, r)_{0,\Gamma_D} - \big(\mu \nabla \boldsymbol{u}^h, \nabla \boldsymbol{w}\big)_{0,\Omega} - \big(\sigma \boldsymbol{u}^h, \boldsymbol{w}\big)_{0,\Omega} + \big(p^h, \nabla \cdot \boldsymbol{w}\big)_{0,\Omega} + \big(\nabla \cdot \boldsymbol{u}^h, r\big)_{0,\Omega} \\ &\quad + J^{h/2}\big(p^h, r\big) + \big(\mu \partial_n \boldsymbol{u}^h, \boldsymbol{w}\big)_{0,\Gamma_D} + \big(\mu \boldsymbol{u}^h, \partial_n \boldsymbol{w}\big)_{0,\Gamma_D} - \big(\gamma_\sigma \mu 2h^{-1} \boldsymbol{u}^h, \boldsymbol{w}\big)_{0,\Gamma_D} \\ &\quad - \big(p^h, \boldsymbol{w} \cdot \boldsymbol{n}\big)_{0,\Gamma_D} - \big(\boldsymbol{u}^h \cdot \boldsymbol{n}, r\big)_{0,\Gamma_D} - \big(\gamma_\sigma 2h^{-1} \boldsymbol{u}^h \cdot \boldsymbol{n}, \boldsymbol{w} \cdot \boldsymbol{n}\big)_{0,\Gamma_D}. \end{aligned} \tag{31}$$

Integrating the term $-(\mu \nabla \boldsymbol{u}^h, \nabla \boldsymbol{w})_{0,\Omega}$ by parts in each element, and using the definition of approximate gradient of pressure (25) we get

$$\begin{aligned} W_1 &= \big(\boldsymbol{f} + \nabla \cdot \mu \nabla \boldsymbol{u}^h - \sigma \boldsymbol{u}^h - \widehat{\nabla} p^h, \boldsymbol{w}\big)_{0,\Omega} + \big(\nabla \cdot \boldsymbol{u}^h, r\big)_{0,\Omega} - \sum_{E \setminus \partial\Omega} \big(\big[\mu \nabla \boldsymbol{u}^h \cdot \boldsymbol{n}\big], \boldsymbol{w}\big)_{0,E} \\ &\quad + \sum_{E \setminus \partial\Omega} \big(\big[p^h\big], \boldsymbol{w} \cdot \boldsymbol{n}\big)_{0,E} + J^{h/2}\big(p^h, r\big) + \big(\boldsymbol{g} + p^h \boldsymbol{n} - \mu \partial_n \boldsymbol{u}^h, \boldsymbol{w}\big)_{0,\Gamma_N} - \big(\boldsymbol{u}_0 - \boldsymbol{u}^h, \mu \partial_n \boldsymbol{w}\big)_{0,\Gamma_D} \\ &\quad + \big(\boldsymbol{u}_0 - \boldsymbol{u}^h, \gamma_\mu \mu 2h^{-1} \boldsymbol{w}\big)_{0,\Gamma_D} + \big(\boldsymbol{u}_0 \cdot \boldsymbol{n} - \boldsymbol{u}^h \cdot \boldsymbol{n}, r\big)_{0,\Gamma_D} + \big(\boldsymbol{u}_0 \cdot \boldsymbol{n} - \boldsymbol{u}^h \cdot \boldsymbol{n}, \gamma_\sigma 2h^{-1} \boldsymbol{w} \cdot \boldsymbol{n}\big)_{0,\Gamma_D}. \end{aligned} \tag{32}$$

We split Eq. (32) into smaller pieces

$$\begin{aligned} Z_1 &:= \big(\boldsymbol{f} + \nabla \cdot \mu \nabla \boldsymbol{u}^h - \sigma \boldsymbol{u}^h - \widehat{\nabla} p^h, \boldsymbol{w}\big)_{0,\Omega}, \\ Z_2 &:= \big(\nabla \cdot \boldsymbol{u}^h, r\big)_{0,\Omega} + J^{h/2}\big(p^h, r\big), \\ Z_3 &:= -\sum_{E \setminus \partial\Omega} \big(\big[\mu \nabla \boldsymbol{u}^h \cdot \boldsymbol{n}\big], \boldsymbol{w}\big)_{0,E} + \sum_{E \setminus \partial\Omega} \big(\big[p^h\big], \boldsymbol{w} \cdot \boldsymbol{n}\big)_{0,E}, \\ Z_4 &:= \big(\boldsymbol{g} + p^h \boldsymbol{n} - \mu \partial_n \boldsymbol{u}^h, \boldsymbol{w}\big)_{0,\Gamma_N}, \\ Z_5 &:= -\big(\boldsymbol{u}_0 - \boldsymbol{u}^h, \mu \partial_n \boldsymbol{w}\big)_{0,\Gamma_D} + \big(\boldsymbol{u}_0 - \boldsymbol{u}^h, \gamma_\mu \mu 2h^{-1} \boldsymbol{w}\big)_{0,\Gamma_D}, \\ Z_6 &:= \big(\boldsymbol{u}_0 \cdot \boldsymbol{n} - \boldsymbol{u}^h \cdot \boldsymbol{n}, r\big)_{0,\Gamma_D} + \big(\boldsymbol{u}_0 \cdot \boldsymbol{n} - \boldsymbol{u}^h \cdot \boldsymbol{n}, \gamma_\sigma 2h^{-1} \boldsymbol{w} \cdot \boldsymbol{n}\big)_{0,\Gamma_D}. \end{aligned}$$

Next we bound the terms Z_i using the Schwarz inequality for both inner products and sums.

$$Z_1 \leqslant \Bigl(\sum_{K\in\mathcal{T}^{h/2}} \bigl(\sigma+\mu h_K^{-2}\bigr)^{-1}\bigl\|\boldsymbol{f}+\nabla\cdot\mu\nabla\boldsymbol{u}^h-\sigma\boldsymbol{u}^h-\widehat{\nabla}p^h\bigr\|_{0,K}^2\Bigr)^{1/2} \times\Bigl(\sum_{K\in\mathcal{T}^{h/2}}\bigl(\sigma+\mu h_K^{-2}\bigr)\|\boldsymbol{w}\|_{0,K}^2\Bigr)^{1/2}, \tag{33}$$

$$Z_2 \leqslant \Bigl(\sum_{K\in\mathcal{T}^{h/2}}\bigl\|\nabla\cdot\boldsymbol{u}^h\bigr\|_{0,K}^2\Bigr)^{1/2}\Bigl(\sum_{K\in\mathcal{T}^{h/2}}\|r\|_{0,K}^2\Bigr)^{1/2}+J^{h/2}\bigl(p^h,p^h\bigr)^{1/2}J^{h/2}(r,r)^{1/2}, \tag{34}$$

$$Z_3 \leqslant \Bigl(\sum_{(E\in\mathcal{T}^{h/2})\backslash\partial\Omega}\mu h_E\bigl\|\bigl[\partial_n\boldsymbol{u}^h\bigr]\bigr\|_{0,E}^2\Bigr)^{1/2}\Bigl(\sum_{(E\in\mathcal{T}^{h/2})\backslash\partial\Omega}\mu h_E^{-1}\|\boldsymbol{w}\|_{0,E}^2\Bigr)^{1/2} + \Bigl(\sum_{(E\in\mathcal{T}^{h/2})\backslash\partial\Omega}h_E\bigl\|\bigl[p^h\bigr]\bigr\|_{0,E}^2\Bigr)^{1/2}\Bigl(\sum_{(E\in\mathcal{T}^{h/2})\backslash\partial\Omega}h_E^{-1}\|\boldsymbol{w}\cdot\boldsymbol{n}\|_{0,E}^2\Bigr)^{1/2}. \tag{35}$$

The term Z_4 is first split into normal and tangential components, see Eq. (2).

$$\begin{aligned} Z_4 &= \bigl(g_n\boldsymbol{n}+\mu\boldsymbol{g}_t-\mu\partial_n\boldsymbol{u}^h+\mu\bigl(\partial_n\boldsymbol{u}^h\cdot\boldsymbol{n}\bigr)\boldsymbol{n}-\mu\bigl(\partial_n\boldsymbol{u}^h\cdot\boldsymbol{n}\bigr)\boldsymbol{n},\boldsymbol{w}-(\boldsymbol{w}\cdot\boldsymbol{n})\boldsymbol{n}+(\boldsymbol{w}\cdot\boldsymbol{n})\boldsymbol{n}\bigr)_{0,\Gamma_N}\\ &= \bigl(g_n+p^h-\mu\partial_n\boldsymbol{u}^h\cdot\boldsymbol{n},\boldsymbol{w}\cdot\boldsymbol{n}\bigr)_{0,\Gamma_N}+\bigl(\mu\boldsymbol{g}_t-\mu\partial_n\boldsymbol{u}^h+\mu\bigl(\partial_n\boldsymbol{u}^h\cdot\boldsymbol{n}\bigr)\boldsymbol{n},\boldsymbol{w}-(\boldsymbol{w}\cdot\boldsymbol{n})\boldsymbol{n}\bigr)_{0,\Gamma_N}\\ &= Z_{4,n}+Z_{4,t}, \end{aligned} \tag{36}$$

$$Z_{4,n} \leqslant \Bigl(\sum_{(E\in\mathcal{T}^{h/2})\cap\Gamma_N}h_E\bigl\|g_n+p^h-\mu\partial_n\boldsymbol{u}^h\cdot\boldsymbol{n}\bigr\|_{0,E}^2\Bigr)^{1/2}\Bigl(\sum_{(E\in\mathcal{T}^{h/2})\cap\Gamma_N}h_E^{-1}\|\boldsymbol{w}\cdot\boldsymbol{n}\|_{0,E}^2\Bigr)^{1/2}, \tag{37}$$

$$Z_{4,t} \leqslant \Bigl(\sum_{(E\in\mathcal{T}^{h/2})\cap\Gamma_N}\mu h_E\bigl\|\boldsymbol{g}_t-\partial_n\boldsymbol{u}^h+\bigl(\partial_n\boldsymbol{u}^h\cdot\boldsymbol{n}\bigr)\boldsymbol{n}\bigr\|_{0,E}^2\Bigr)^{1/2}\Bigl(\sum_{(E\in\mathcal{T}^{h/2})\cap\Gamma_N}\mu h_E^{-1}\|\boldsymbol{w}\|_{0,E}^2\Bigr)^{1/2}, \tag{38}$$

$$Z_5 \leqslant \Bigl(\sum_{(E\in\mathcal{T}^{h/2})\cap\Gamma_D}\mu h_E^{-1}\bigl\|\boldsymbol{u}_0-\boldsymbol{u}^h\bigr\|_{0,E}^2\Bigr)^{1/2}\Bigl(\sum_{(E\in\mathcal{T}^{h/2})\cap\Gamma_D}\mu h_E\|\partial_n\boldsymbol{w}\|_{0,E}^2\Bigr)^{1/2} + \Bigl(\sum_{(E\in\mathcal{T}^{h/2})\cap\Gamma_D}\mu h_E^{-1}\bigl\|\boldsymbol{u}_0-\boldsymbol{u}^h\bigr\|_{0,E}^2\Bigr)^{1/2}\Bigl(\sum_{(E\in\mathcal{T}^{h/2})\cap\Gamma_D}\mu h_E^{-1}\|\boldsymbol{w}\|_{0,E}^2\Bigr)^{1/2}, \tag{39}$$

$$Z_6 \leqslant \Bigl(\sum_{(E\in\mathcal{T}^{h/2})\cap\Gamma_D}h_E^{-1}\bigl\|\boldsymbol{u}_0\cdot\boldsymbol{n}-\boldsymbol{u}^h\cdot\boldsymbol{n}\bigr\|_{0,E}^2\Bigr)^{1/2}\Bigl(\sum_{(E\in\mathcal{T}^{h/2})\cap\Gamma_D}h_E\|r\|_{0,E}^2\Bigr)^{1/2} + \Bigl(\sum_{(E\in\mathcal{T}^{h/2})\cap\Gamma_D}h_E^{-1}\bigl\|\boldsymbol{u}_0\cdot\boldsymbol{n}-\boldsymbol{u}^h\cdot\boldsymbol{n}\bigr\|_{0,E}^2\Bigr)^{1/2}\Bigl(\sum_{(E\in\mathcal{T}^{h/2})\cap\Gamma_D}h_E^{-1}\|\boldsymbol{w}\cdot\boldsymbol{n}\|_{0,E}^2\Bigr)^{1/2}. \tag{40}$$

By the interpolation estimate (29) and since $(\boldsymbol{u}^h, p^h)$ has same values on both meshes, we find that

$$W_1 \leqslant C\Bigl(\sum_{K\in\mathcal{T}^{h/2}}E_K\bigl[\bigl(\boldsymbol{u}^h,p^h\bigr)\bigr]^2\Bigr)^{1/2} \leqslant C\Bigl(\sum_{K\in\mathcal{T}^{h}}E_K\bigl[\bigl(\boldsymbol{u}^h,p^h\bigr)\bigr]^2\Bigr)^{1/2}. \tag{41}$$

Step 3. Now we have bounded the term W_1 and next we bound the term W_2. Since both $(\boldsymbol{u}^h, p^h)$ and $(\boldsymbol{u}^{h/2}, p^{h/2})$ are solutions to the problem on different meshes, we get

$$W_2 = L^{h/2}\bigl[\bigl(\boldsymbol{v}^h,q^h\bigr)\bigr]-B^{h/2}\bigl[\bigl(\boldsymbol{u}^h,p^h\bigr),\bigl(\boldsymbol{v}^h,q^h\bigr)\bigr]-L^h\bigl[\bigl(\boldsymbol{v}^h,q^h\bigr)\bigr]+B^h\bigl[\bigl(\boldsymbol{u}^h,p^h\bigr),\bigl(\boldsymbol{v}^h,q^h\bigr)\bigr]. \tag{42}$$

Below we will denote with subscripts h and $h/2$ the mesh that we are currently integrating on, e.g. $(\cdot,\cdot)_{0,\Gamma_{D,h}}$. Since $(\boldsymbol{u}^h, p^h)$ and $(\boldsymbol{v}^h, q^h)$ have same values on both meshes, we have

$$\begin{aligned}W_2 &= J^h(p^h,q^h) - J^{h/2}(p^h,q^h) + \left(\boldsymbol{u}^h - \boldsymbol{u}_0, \gamma_\mu \mu h^{-1}\boldsymbol{v}^h\right)_{0,\Gamma_{D,h}} + \left(\boldsymbol{u}^h\cdot\boldsymbol{n} - \boldsymbol{u}_0\cdot\boldsymbol{n}, \gamma_\sigma h^{-1}\boldsymbol{v}^h\cdot\boldsymbol{n}\right)_{0,\Gamma_{D,h}}\\ &\quad - \left(\boldsymbol{u}^h - \boldsymbol{u}_0, \gamma_\mu \mu 2h^{-1}\boldsymbol{v}^h\right)_{0,\Gamma_{D,h/2}} - \left(\boldsymbol{u}^h\cdot\boldsymbol{n} - \boldsymbol{u}_0\cdot\boldsymbol{n}, \gamma_\sigma 2h^{-1}\boldsymbol{v}^h\cdot\boldsymbol{n}\right)_{0,\Gamma_{D,h/2}}\\ &= J^{h/2}(p^h,q^h) - \left(\boldsymbol{u}^h - \boldsymbol{u}_0, \gamma_\mu \mu h^{-1}\boldsymbol{v}^h\right)_{0,\Gamma_{D,h/2}} - \left(\boldsymbol{u}^h\cdot\boldsymbol{n} - \boldsymbol{u}_0\cdot\boldsymbol{n}, \gamma_\sigma h^{-1}\boldsymbol{v}^h\cdot\boldsymbol{n}.\right)_{0,\Gamma_{D,h/2}}. \end{aligned} \tag{43}$$

Using the Schwarz inequality we obtain

$$\begin{aligned}W_2 \leqslant C\Bigg[& J^{h/2}(p^h,p^h)^{1/2} J^{h/2}(q^h,q^h)^{1/2}\\ &+ \Bigg(\sum_{(E\in\mathcal{T}^{h/2})\cap\Gamma_D} \mu h_E^{-1}\|\boldsymbol{u}^h - \boldsymbol{u}_0\|_{0,E}^2\Bigg)^{1/2}\Bigg(\sum_{(E\in\mathcal{T}^{h/2})\cap\Gamma_D} \mu h_E^{-1}\|\boldsymbol{v}^h\|_{0,E}^2\Bigg)^{1/2}\\ &+ \Bigg(\sum_{(E\in\mathcal{T}^{h/2})\cap\Gamma_D} h_E^{-1}\|\boldsymbol{u}^h\cdot\boldsymbol{n} - \boldsymbol{u}_0\cdot\boldsymbol{n}\|_{0,E}^2\Bigg)^{1/2}\Bigg(\sum_{(E\in\mathcal{T}^{h/2})\cap\Gamma_D} h_E^{-1}\|\boldsymbol{v}^h\cdot\boldsymbol{n}\|_{0,E}^2\Bigg)^{1/2}\Bigg]. \end{aligned} \tag{44}$$

Since $\|(\boldsymbol{v}^{h/2}, q^{h/2})\|_{h/2} = 1$ the stability of the interpolate gives

$$W_2 \leqslant C\Bigg(\sum_{K\in\mathcal{T}^{h/2}} E_K\big[(\boldsymbol{u}^h,p^h)\big]^2\Bigg)^{1/2} \leqslant C\Bigg(\sum_{K\in\mathcal{T}^{h}} E_K\big[(\boldsymbol{u}^h,p^h)\big]^2\Bigg)^{1/2}. \tag{45}$$

Step 4. Now all the pieces are ready and we only need to combine Eqs. (30), (41) and (45) to get the desired result. □

5. Numerical examples

In this section we illustrate the method and analytical results with numerical examples. We concentrate on showing that the results derived in the previous sections hold with viscosity $\mu \geqslant 0$, including Darcy limit $\mu = 0$. Furthermore, we compare the results with the traditional boundary conditions.

Our model problem is

$$\begin{aligned}&\boldsymbol{u} - \nabla\cdot\mu\nabla\boldsymbol{u} + \nabla p = 0 \quad \text{in } \Omega,\\ &\nabla\cdot\boldsymbol{u} = 0 \quad \text{in } \Omega.\end{aligned}$$

First we compute the convergence rate of the error in the energy norm with different values of viscosity μ. Our domain Ω is the unit square with Dirichlet boundary conditions computed from the known exact solution;

$$\begin{aligned}&p = -\sin(x)\sinh(y) - \big(\cos(1)-1\big)\big(\cosh(1)-1\big) \quad \text{and}\\ &\boldsymbol{u} = -\nabla p = \begin{pmatrix}\cos(x)\sinh(y)\\ \sin(x)\cosh(y)\end{pmatrix}.\end{aligned}$$

Since the pressure p is harmonic, the solution is independent of the viscosity. In all the subsequent computations Nitsche stability parameters are $\gamma_\mu = 10$ and $\gamma_\sigma = 1$. In Fig. 1 are the convergence rates of the method. We see that the convergence rate is $\mathcal{O}(h)$ with all the values of viscosity, even on Darcy limit, as predicted by Lemma 4.2. In Fig. 2 are the a posteriori estimators computed for the same problem with the same uniformly refined meshes. We see that also the a posteriori error estimator converges with the same rate as the exact error. Only at the Darcy limit $\mu = 0$ we see a slight reduction in the convergence rate.

Next we compare the Nitsche method to the traditional boundary conditions. Here our domain is the unit square and we use the following boundary conditions

$$\begin{aligned}&\boldsymbol{u} = \boldsymbol{0} && \text{on } \big\{x\in(0,1),\ y=0\big\} \text{ and } \big\{x\in(0,1),\ y=1\big\},\\ &g_n = 1,\quad \boldsymbol{g}_t = \boldsymbol{0} && \text{on } \big\{x=0,\ y\in(0,1)\big\},\\ &g_n = 0,\quad \boldsymbol{g}_t = \boldsymbol{0} && \text{on } \big\{x=1,\ y\in(0,1)\big\}.\end{aligned}$$

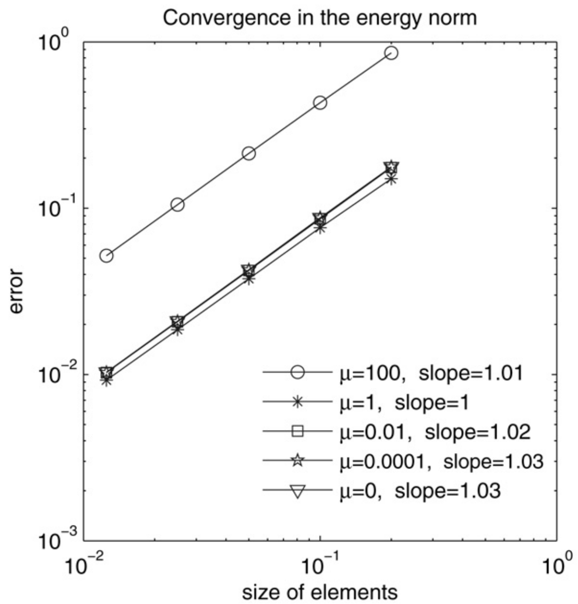

Fig. 1. The convergence of the error in the energy norm for various values of viscosity parameter. The convergence rates are given in the legend. Notice that even the Darcy limit case ($\mu = 0$) converges with the optimal rate of $\mathcal{O}(h)$.

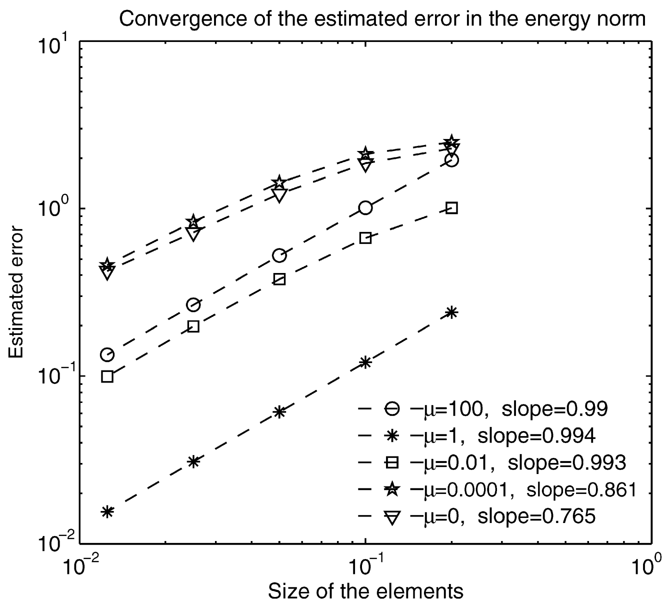

Fig. 2. The convergence of the a posteriori estimator for various values of viscosity parameter. The convergence rates are given in the legend. The convergence rates are the same as for the exact error, see the figure above.

In Fig. 3 are the velocities with different values of viscosity. We see that the traditional method cannot produce slip boundary conditions of the Darcy problem unless the viscosity is equal to zero. On the other hand, Nitsche's method moves continuously towards the slip boundary conditions as the viscosity diminishes. In Fig. 4 we have the velocity profile in x-direction at line $x = 0.5$. We notice that the traditional method has oscillations in the velocity near the boundaries in the case of small viscosity. In Fig. 5 we have the velocity in y-direction at same line $x = 0.5$. The velocity in y-direction should be zero, but with traditional boundary conditions and with small viscosity there is also oscillation in the velocity in y-direction. These oscillations are due to the fact that the problem is very close to Darcy

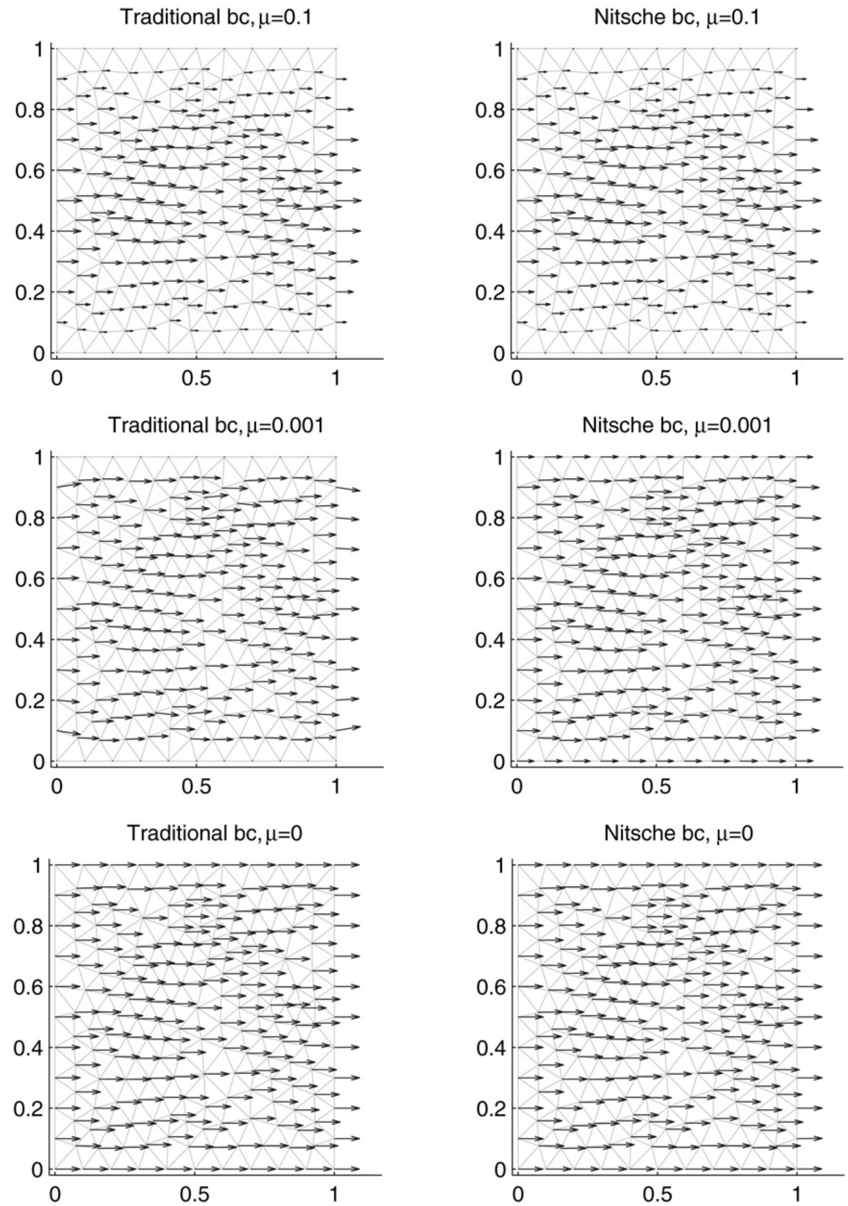

Fig. 3. Velocity fields of the model problem, on the left using the traditional and on the right using Nitsche boundary conditions. From top to bottom viscosity μ has values 0.1, 0.001, and 0. The lengths of the vectors are scaled differently on each row. For size of the velocity, see the velocity profile figures below. Notice the difference in the solutions near the boundaries on the middle row.

problem but the traditional way of prescribing the boundary conditions does not allow slip in tangential direction before the viscosity is equal to zero.

We think that the previous example clearly illustrates the shortcoming of the traditional boundary conditions in the Brinkman problem; the whole range of viscosity cannot be used. From the non-physical oscillations it is obvious that the results are not accurate or reliable near the boundaries with the traditional no-slip boundary conditions if the viscosity is small. Refining the mesh pushes the inaccuracy closer to the boundary but will not remove the problem. Nitsche's method handles these difficulties even on a coarse mesh.

Finally we test the adaptive refinement based on the elementwise a posteriori error estimator. The domain is the unit square and we use the Dirichlet boundary conditions computed from the known exact solution. The exact solution (in the polar coordinates) is

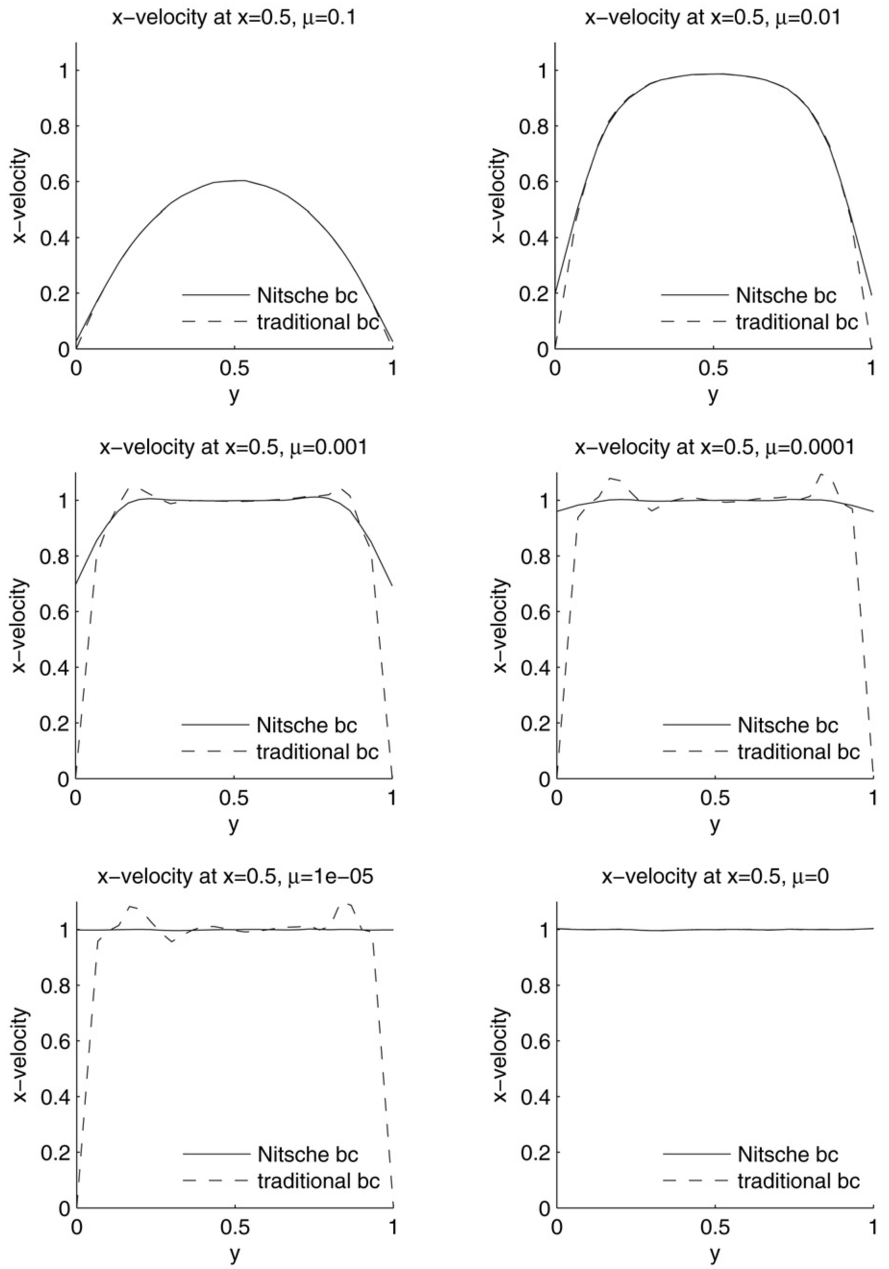

Fig. 4. The velocity profile to x-direction at line $x = 0.5$ with different values of viscosity μ. The solid line is computed with Nitsche boundary conditions and the dashed line with the traditional boundary conditions. Notice the oscillations with the traditional method near the boundary with small μ.

$$p = -r^{\beta}\sin(\beta\theta) + \frac{2\sin(\pi\beta/4)(2^{\beta/2} + \sin(\pi\beta/4))}{2 + 3\beta + \beta^2} \quad \text{and}$$

$$\boldsymbol{u} = -\nabla p = \beta r^{\beta-1}\begin{pmatrix} -\sin(\theta - \beta\theta) \\ \cos(\theta - \beta\theta) \end{pmatrix},$$

where $\beta > 0$ is a parameter. With the parameter β we can adjust the smoothness of the solution so that $p \in H^{\beta+1}(\Omega)$ and $\boldsymbol{u} \in [H^{\beta}(\Omega)]^2$. With $\beta > 1$ we assume we have a solution but the a priori result, Lemma 4.2, is no longer applicable. In Fig. 6 we have the first three rounds of adaptive refinement for $\beta = 1.3$ and $\mu = 1$. We see that the

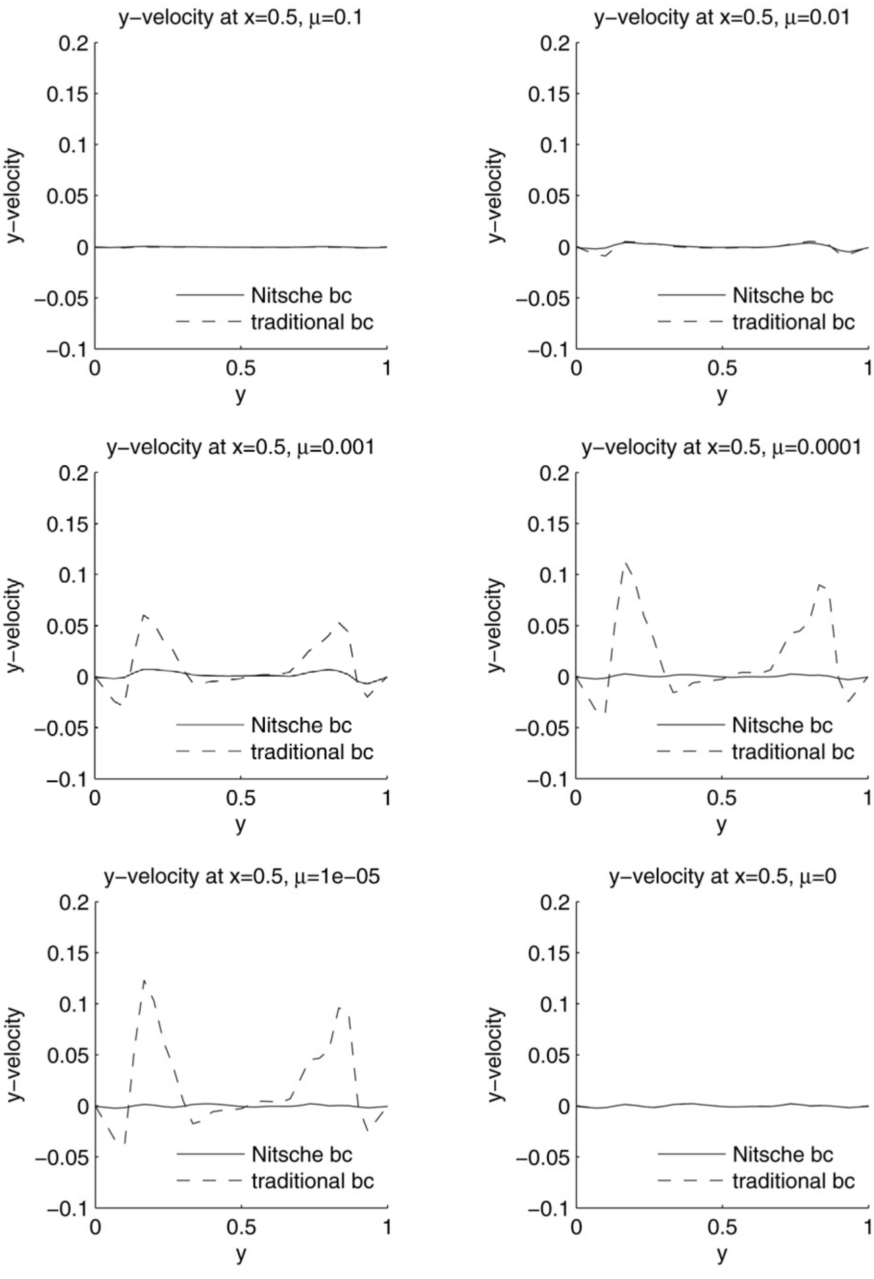

Fig. 5. The velocity profile to y-direction at line $x = 0.5$ with different values of viscosity μ. The solid line is computed with Nitsche boundary conditions and the dashed line with the traditional boundary conditions. Notice the oscillations with the traditional method near the boundary with small μ.

a posteriori estimator detects the singularity at the origin and refines there. In the same Fig. 6 we also have the same problem with $\mu = 0.001$. In this case the a posteriori indicator has problems in seeing the singularity at the origin and refines also on the boundaries. In both cases the ratio between the estimated and the exact error stays constant which is perhaps the most important feature for an a posteriori estimator.

Looking at Figs. 2 and 6 we see that the a posteriori indicator is less sharp near the Darcy limit. This is because the residual inside the elements in the a posteriori estimator is of the form $\|\boldsymbol{u}^h + \widehat{\nabla} p^h\|_{0,K}^2$ if the viscosity and load are zero (or very small). More precisely, there are no powers of h in the coefficient; therefore the approximate negative gradient of pressure $-\widehat{\nabla} p^h$ has to be close to the velocity. The problem is worse near the boundaries since the approximate

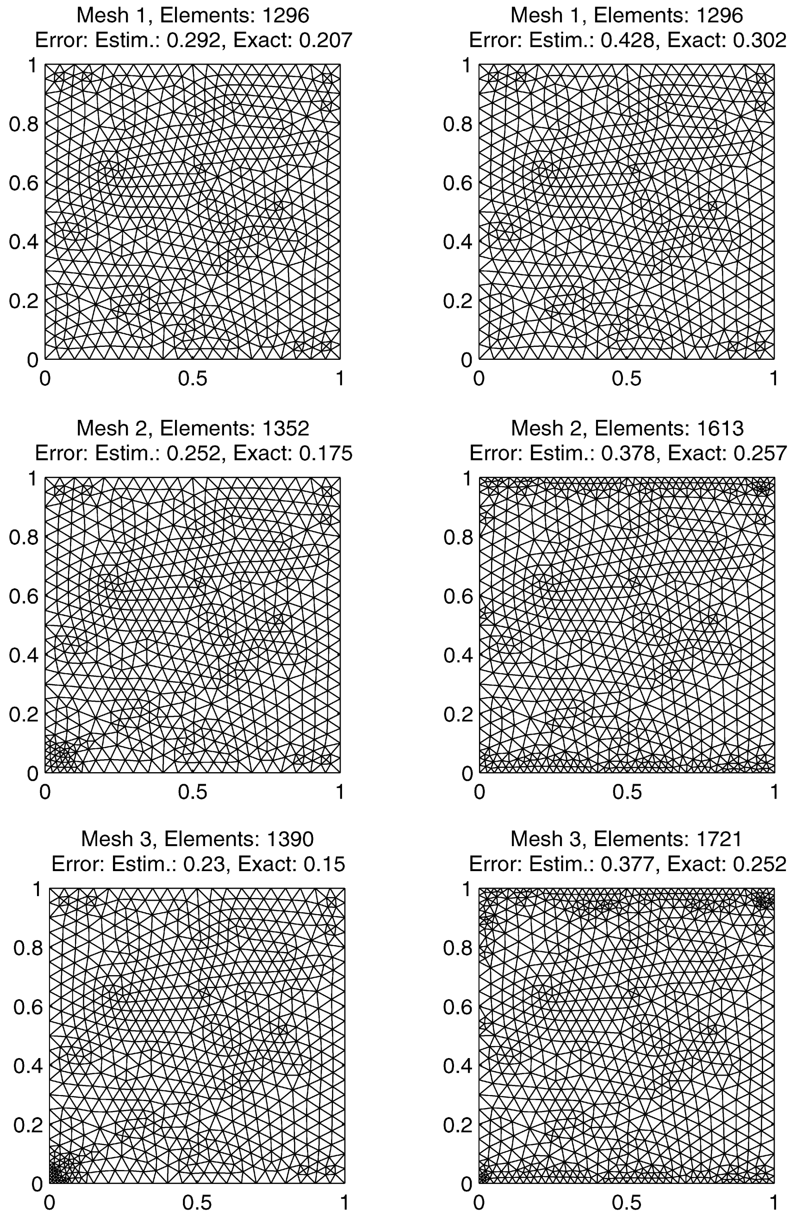

Fig. 6. First three rounds of adaptive refinement based on the a posteriori estimator. On the left we have $\mu = 1$ and on the right $\mu = 0.001$. There is a singularity at the origin. With smaller viscosity the a posteriori estimator has problems finding the singularity. This is because the reconstructed gradient of the pressure has larger role with small viscosity and near the boundaries the reconstruction is not as sharp as inside the domain. Still, the ratio between the exact error and the estimator stays almost constant which is important for the estimator.

gradient is essentially computed from the pressure jumps, and on the boundary we do not have a value for the jump. With larger viscosity the reconstruction is not as crucial anymore since we have powers of h in the coefficient reducing the residual if the elements are small.

References

[1] Y. Bazilevs, T.J.R. Hughes, Weak imposition of Dirichlet boundary conditions in fluid mechanics, Computers & Fluids 36 (1) (2007) 12–26.
[2] S. Brenner, L. Scott, The Mathematical Theory of Finite Element Methods, Springer, New York, 1994.

[3] E. Burman, A unified analysis for conforming and nonconforming stabilized finite element methods using interior penalty, SIAM Journal on Numerical Analysis 43 (5) (2005) 2012–2033.
[4] E. Burman, Pressure projection stabilizations for Galerkin approximations of Stokes' and Darcy's problem, Numerical Methods for Partial Differential Equations 24 (1) (2008) 127–143.
[5] E. Burman, M.A. Fernández, P. Hansbo, Continuous interior penalty finite element method for Oseen's equations, SIAM Journal on Numerical Analysis 44 (3) (2006) 1248–1274.
[6] E. Burman, P. Hansbo, A unified stabilized method for Stokes' and Darcy's equations, Journal of Computational and Applied Mathematics 198 (1) (2007) 35–51.
[7] J. Freund, R. Stenberg, On weakly imposed boundary conditions for second order problems, in: M. Morandi Cecchi, et al. (Eds.), Proceedings of the Ninth Int. Conf. Finite Elements in Fluids, Venice, 1995, pp. 327–336.
[8] T.J.R. Hughes, L. Franca, A new finite element formulation for CFD: VII. The Stokes problem with various well-posed boundary conditions: Symmetric formulations that converge for all velocity/pressure spaces, Computer Methods in Applied Mechanics and Engineering 65 (1) (1987) 85–96.
[9] K. Mardal, X. Tai, R. Winther, A robust finite element method for Darcy–Stokes flow, SIAM Journal on Numerical Analysis 58 (5) (2002) 1605–1631.
[10] J. Nitsche, Über ein Variationsprinzip zur Lösung von Dirichlet-Problemen bei Verwendung von Teilräumen, die keinen Randbedingungen unterworfen sind, Abhandlungen aus dem Mathematischen Seminar der Universität Hamburg 36 (1971) 9–15.
[11] V. Thomée, Galerkin Finite Element Methods for Parabolic Problems, Springer, Berlin, 1997.